# Studies on Mixed Metal(II)–Iron(II) Chloride Systems. Part 1. Mössbauer and *X*-Ray Powder Diffraction Data for $M_xFe_{1-x}Cl_2\cdot4H_2O$ (M = Mn, Co, or Ni; $x$ = 0—0.75) Systems †

**Bella Y. Enwiya and Jack Silver** *
*Department of Chemistry, University of Essex, Wivenhoe Park, Colchester CO4 3SQ*
**Ian E. G. Morrison**
*Department of Chemistry, Imperial College, London SW7 2AZ*

The $^{57}$Fe Mössbauer data of the phases $M_xFe_{1-x}Cl_2\cdot4H_2O$ (M = Mn, Co, or Ni; $x$ = 0—0.75) are presented. The quadrupole splittings decrease significantly in the Fe–Co and Fe–Ni systems. These changes are explained in terms of changes in site symmetry resulting in a change of orbital occupancy from $d_{xy}$ to $d_{xz}$, $d_{yz}$. The changes in site symmetry are caused by changes in Fe–$OH_2$ bonding in the lattices ' squeezing ' the $Fe^{II}$ centres. The Fe–Mn system also gives results which appear to be directly related to volume change, but no evidence is found for pressure effects. The temperature dependence of the quadrupole splitting in the Fe–Mn system is discussed. It is mainly due to the Boltzmann population of the $d^6$ manifolds.

There have been extensive reports in the literature of Mössbauer spectroscopic studies on iron(II) chloride hydrates.[1–23]

The crystal structures of $FeCl_2\cdot2H_2O$ and $FeCl_2\cdot4H_2O$ are known [24,25] and the Mössbauer data for these materials have been explained on the basis of their structures.[2,7–10,16–23] Several workers have established that for $FeCl_2\cdot4H_2O$ the quadrupole coupling constant $e^2qQ$ is positive [1,7,16] and the orientation of the electric field gradient tensor at the iron nucleus in a single crystal field of $FeCl_2\cdot4H_2O$ has been determined. The principal axis of the tensor lies close to the Fe–Cl bonds of the *trans*-octahedral $FeCl_2(H_2O)_4$ unit, the minor axes being directed between the Fe–O bonds.[16]

We have reported the preparation [26] and Mössbauer data for $KFe_xM_{1-x}F_3$ (M = Mn, Co, Ni, and Zn; $x$ = 0.5) [27] which show spectra with fundamental differences to that of $KFeF_3$.[28–31] The results obtained were subtly different from the high-pressure work reported by Drickamer and co-workers [30] and indicated that squeezing of Fe in the $KFe_{0.5}M_{0.5}F_3$ (M = Co or Ni) lattice could not account for the observed small quadrupole splittings. It was apparent that the small changes were more likely to be caused by interactions with the other transition metals in the perovskite lattice.[27] In the light of these novel results in the fluorides it was thought worthwhile to investigate the mixed chloride hydrate systems.

We now report *X*-ray powder diffraction and Mössbauer spectroscopic studies of the systems $M_xFe_{1-x}Cl_2\cdot4H_2O$ (M = Mn, Co, or Ni; $x$ = 0—0.75). Manganese was chosen as $Mn^{II}$ is larger than $Fe^{II}$, whereas $Co^{II}$ and $Ni^{II}$ are both smaller.

## Experimental

The materials were all prepared by the same method using the appropriate mol ratios for the required material; for example, for $Mn_{0.5}Fe_{0.5}Cl_2\cdot4H_2O$, 1 : 1 mol ratios of $FeCl_2\cdot4H_2O$ and $MnCl_2\cdot4H_2O$ were used. A solution of $FeCl_2\cdot4H_2O$ was boiled with a small amount of ascorbic acid (present as a reducing agent against $Fe^{III}$) and a solution of the appropriate transition metal chloride added. The resulting solution was heated to dryness in an $N_2$ atmosphere. Analytical data for the $M_{0.5}Fe_{0.5}Cl_2\cdot4H_2O$ (M = Co, Ni, or Mn) phases appear in

† *Non-S.I. unit employed*: 1 Ci = 3.7 × $10^{10}$ Bq.

**Table 1.** Analytical results for $M_{0.5}Fe_{0.5}Cl_2\cdot4H_2O$ phases (M = Mn, Co, or Ni)

| | Analysis * (%) | | |
|---|---|---|---|
| Phase | Fe | M | Cl |
| $Mn_{0.5}Fe_{0.5}Cl_2\cdot4H_2O$ | 13.90 (14.05) | 13.80 (13.85) | 35.50 (33.75) |
| $Co_{0.5}Fe_{0.5}Cl_2\cdot4H_2O$ | 13.80 (13.95) | 14.80 (14.70) | 35.40 (35.40) |
| $Ni_{0.5}Fe_{0.5}Cl_2\cdot4H_2O$ | 13.90 (13.95) | 14.70 (14.65) | 35.40 (35.40) |

* Calculated values in parentheses.

**Table 2.** $^{57}$Fe Mössbauer parameters for high-spin iron(II) halides

| Compound | $T$/K | $\delta$/ mm s$^{-1}$ | $\Delta$/ mm s$^{-1}$ | $\Gamma$/ mm s$^{-1}$ |
|---|---|---|---|---|
| $FeCl_2\cdot4H_2O$ | 298 | 1.219(1) | 2.996(3) | 0.14(1) |
| $Co_{0.17}Fe_{0.83}Cl_2\cdot4H_2O$ | 298 | 1.217(2) | 2.997(4) | 0.13(1) |
| $Co_{0.20}Fe_{0.80}Cl_2\cdot4H_2O$ | 298 | 1.219(2) | 2.997(3) | 0.14(1) |
| $Co_{0.25}Fe_{0.75}Cl_2\cdot4H_2O$ | 298 | 1.218(2) | 2.995(5) | 0.14(1) |
| $Co_{0.33}Fe_{0.67}Cl_2\cdot4H_2O$ | 298 | 1.216(2) | 3.001(4) | 0.13(1) |
| $Co_{0.5}Fe_{0.5}Cl_2\cdot4H_2O$ | 298 | 1.193(2) | 1.556(4) | 0.11(1) |
| | 80 | 1.314(1) | 1.661(2) | 0.13(1) |
| $Co_{0.75}Fe_{0.25}Cl_2\cdot xH_2O$ | 298 | 1.21(1) | 1.55(1) | 0.11(1) |
| | | 1.21(1) | 2.65(1) | 0.23(1) |
| $Ni_{0.75}Fe_{0.25}Cl_2\cdot xH_2O$ | 298 | 1.205(2) | 2.580(7) | 0.13(1) |
| | | 1.188(8) | 1.61(2) | 0.10(1) |
| $Ni_{0.5}Fe_{0.5}Cl_2\cdot4H_2O$ | 298 | 1.190(6) | 1.571(11) | 0.11(1) |
| | 80 | 1.313(2) | 1.691(4) | 0.12(1) |
| $Ni_{0.25}Fe_{0.75}Cl_2\cdot4H_2O$ | 298 | 1.219(1) | 2.997(3) | 0.14(1) |
| $Mn_{0.25}Fe_{0.75}Cl_2\cdot4H_2O$ | 298 | 1.218(2) | 2.997(3) | 0.14(1) |
| $Mn_{0.75}Fe_{0.25}Cl_2\cdot4H_2O$ | 298 | 1.21(2) | 2.63(3) | 0.12(1) |
| | 80 | 1.341(2) | 3.291(3) | 0.12(1) |
| | 100 | 1.331(2) | 3.265(4) | 0.12(1) |
| | 125 | 1.317(2) | 3.221(3) | 0.12(1) |
| | 150 | 1.305(2) | 3.178(3) | 0.13(1) |
| | 175 | 1.287(2) | 3.103(4) | 0.12(1) |
| $Mn_{0.50}Fe_{0.50}Cl_2\cdot4H_2O$ | 200 | 1.272(2) | 3.025(5) | 0.12(1) |
| | 225 | 1.256(2) | 3.946(4) | 0.12(1) |
| | 250 | 1.242(3) | 2.838(5) | 0.12(1) |
| | 275 | 1.222(2) | 2.735(4) | 0.12(1) |
| | 300 | 1.202(3) | 2.595(5) | 0.12(1) |
| | 325 | 1.164(4) | 2.370(7) | 0.13(1) |
| | 350 | 1.132(4) | 2.272(8) | 0.12(1) |

**Table 3.** *X*-Ray diffraction powder data [a]

| $FeCl_2·4H_2O$ | | | | $Co_{0.5}Fe_{0.5}Cl_2·4H_2O$ | | $Ni_{0.5}Fe_{0.5}Cl_2·4H_2O$ | | $MnCl_2·4H_2O$ | | | | $Mn_{0.5}Fe_{0.5}Cl_2·4H_2O$ | |
|---|---|---|---|---|---|---|---|---|---|---|---|---|---|
| Intensity | $d_{obs.}$/Å | $d_{calc.}$[b]/Å | *hkl* | $d_{obs.}$[c]/Å | Intensity | $d_{obs.}$[c]/Å | Intensity | Intensity | $d_{obs.}$/Å | $d_{calc.}$[d]/Å | *hkl* | $d_{obs.}$[e]/Å | Intensity |
| s | 5.52 | 5.47 | 100 | 5.52 | s | 5.50 | s | ms | 5.52 | 5.511 | $11\bar{1}$ | 5.55 | ms |
| s | 5.35 | 5.29 | 011, $01\bar{1}$ | 5.32 | s | 5.31 | s | s | 4.94 | 4.921 | 011, $01\bar{1}$ | 4.89 | ms |
| s | 4.39 | 4.401 | $11\bar{1}$ | 4.36 | ms | 4.35 | ms | m | 4.76 | 4.775 | 020 | 4.73 | w |
| s | 3.97 | 3.962 | $10\bar{2}$ | 3.96 | s | 3.95 | s | vs | 4.43 | 4.487 | 101 | 4.39 | s |
| m | 3.57 | 3.585 | 020 | | | | | vvw | 4.28 | 4.418 | $21\bar{1}$ | 4.22 | vvw |
| m | 3.51 | 3.468 | $11\bar{2}$ | 3.48 | m | 3.48 | m | vvw | 4.20 | 4.387 | 120 | 4.12 | vvw |
| | | 3.435 | 012, $01\bar{2}$ | 3.43 | m | 3.44 | m | w | 4.05 | 4.061 | 111 | 4.03 | vw |
| s | 3.06 | 3.016 | $12\bar{1}$ | 3.00 | s | 3.00 | s | vw | 3.52 | 3.524 | $31\bar{1}$ | 3.49 | w |
| vvw | 2.99 | 3.000 | 120 | 2.94 | vvw | 2.93 | vvw | vvw | 3.44 | 3.447 | $22\bar{1}$ | 3.25 | vvw |
| m | 2.78 | 2.788 | $20\bar{2}$ | 2.78 | m | 2.77 | m | w | 3.27 | 3.270 | 121 | 3.19 | vvw |
| w | 2.71 | 2.736 | 102 | 2.72 | w | 2.72 | w | vw | 3.21 | 3.224 | 211 | | |
| w | 2.67 | 2.658 | $12\bar{2}$ | 2.66 | w | 2.65 | w | s | 3.05 | 3.060 | $\bar{1}30$ | 3.03 | s |
| vvw | 2.61 | 2.600 | $21\bar{2}$ | 2.61 | w | 2.61 | w | vs | 2.92 | 2.912 | $11\bar{2}$ | 2.89 | vs |
| vvw | 2.56 | 2.559 | 210 | 2.56 | vvw | 2.55 | vvw | vw | 2.82 | 2.819 | $13\bar{1}$ | 2.80 | ms |
| w | 2.53 | 2.556 | 112 | 2.51 | vvw | 2.51 | vvw | s | 3.76 | 2.762 | 230 | 2.74 | ms |
| vvw | 2.49 | 2.451 | 013, $01\bar{3}$ | 2.47 | vvw | 2.47 | vvw | m | 2.70 | 2.702 | 301 | 2.69 | m |
| vs | 2.27 | 2.280 | $22\bar{1}$ | 2.19 | vs | 2.19 | vs | s | 2.59 | 2.596 | 131 | 2.57 | m |
| vs | 2.25 | 2.267 | $21\bar{3}$ | 2.17 | vs | 2.18 | vs | ms | 2.48 | 2.491 | $40\bar{2}$ | 2.47 | vw |
| ms | 2.19 | 2.197 | $13\bar{1}$ | 2.12 | ms | 2.11 | ms | vvw | 2.44 | 2.438 | $33\bar{1}$ | 2.42 | vvw |
| w | 2.13 | 2.110 | $10\bar{4}$ | | | | | vvw | 2.40 | 2.401 | 420 | 2.38 | vvw |
| vvw | 2.11 | 2.109 | 023, $02\bar{3}$ | | | | | vw | 2.34 | 2.334 | 140 | 2.33 | vvw |
| vvw | 2.062 | 2.046 | $13\bar{2}$ | 2.047 | vvw | 2.045 | vvw | w | 2.21 | 2.209 | $42\bar{2}$ | 2.20 | vw |
| vvw | 2.040 | 2.040 | 032, $03\bar{2}$ | 2.025 | vvw | 2.023 | vvw | w | 2.20 | 2.195 | $23\bar{2}$ | 2.18 | vw |
| vvw | 2.019 | 2.024 | $11\bar{4}$ | | | | | vw | 2.14 | 2.152 | 411 | 2.13 | vw |
| w | 1.980 | 1.988 | $22\bar{3}$ | 1.979 | vvw | 1.977 | vvw | m | 2.051 | 2.060 | 331 | 2.042 | m |
| vvw | 1.965 | 1.960 | $30\bar{2}$ | 1.959 | vvw | 1.957 | vvw | vvw | 2.025 | 2.021 | $30\bar{3}$ | 2.014 | vw |
| | | 1.948 | 221 | 1.939 | vvw | 1.937 | vvw | w | 1.999 | 1.998 | 132 | 1.998 | w |
| vvw | 1.937 | 1.930 | 202 | 1.912 | vvw | 1.910 | v | m | 1.975 | 1.977 | $31\bar{3}$ | 1.967 | m |
| vvw | 1.918 | 1.901 | $21\bar{4}$ | | | | | m | 1.901 | 1.906 | $53\bar{1}$ | 1.889 | m |
| m | 1.899 | 1.891 | $31\bar{2}$ | 1.840 | w | 1.888 | w | m | 1.879 | 1.877 | 013, $01\bar{3}$ | 1.868 | vw |
| vw | 1.877 | 1.880 | $31\bar{1}$ | 1.864 | vvw | 1.862 | vvw | vvw | 1.836 | 1.836 | 042, $04\bar{2}$ | 1.826 | vw |
| w | 1.855 | 1.858 | $23\bar{1}$ | 1.850 | vvw | 1.849 | vvw | w | 1.809 | 1.809 | 322 | 1.806 | vw |
| vvw | 1.834 | 1.827 | 300 | 1.832 | m | 1.831 | m | vvw | 1.779 | 1.777 | 023, $02\bar{3}$ | 1.773 | vvw |
| vvw | 1.814 | 1.815 | $23\bar{2}$ | 1.812 | vw | 1.811 | vw | vvw | 1.757 | 1.757 | 151 | 1.751 | vvw |
| w | 1.791 | 1.793 | 040 | 1.792 | w | 1.794 | w | vvw | 1.740 | 1.733 | 521 | 1.737 | vvw |
| vw | 1.575 | 1.572 | 213 | | | | | | | | | | |
| w | 1.565 | 1.565 | 133 | 1.531 | w | 1.530 | w | | | | | | |

[a] $d$/Å = interlayer spacing. [b] The $FeCl_2·4H_2O$ phase is fitted to the lattice parameters given in ref. 25. [c] $Ni_{0.5}Fe_{0.5}Cl_2·4H_2O$ and $Co_{0.5}Fe_{0.5}Cl_2·4H_2O$ are similar both in intensity and $d$/Å to $FeCl_2·4H_2O$. From a visual comparison of the data both the new phases show smaller cells than that of $FeCl_2·4H_2O$. However, the cell sizes of these new phases have not been uniquely established as both the cell constants and cell angles can be varied to fit the data. [d] The $MnCl_2·4H_2O$ phase is fitted to the lattice parameters given in ref. 38. [e] The data for $Fe_{0.5}Mn_{0.5}Cl_2·4H_2O$ are similar to those of $MnCl_2·4H_2O$, although the cell size (from a visual inspection) is clearly smaller. Because both the cell constants and cell angles could be varied to fit the data the cell size of this new phase has not been uniquely determined.

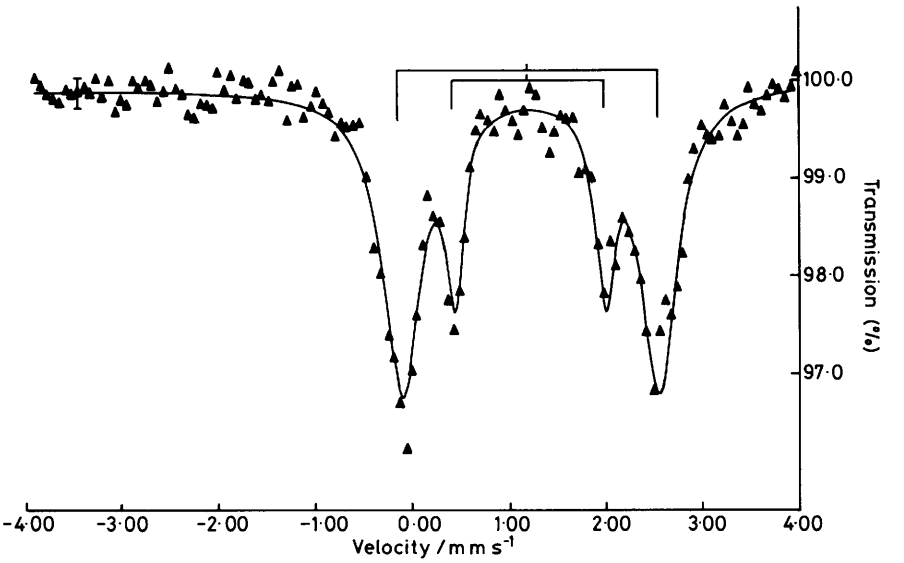


**Figure 1.** $^{57}$Fe Mössbauer spectrum of $Co_{0.75}Fe_{0.25}Cl_2 \cdot xH_2O$ phase (see text) at 298 K: $\delta = 1.21(1)$, $\Delta = 2.65(1)$, $\Gamma = 0.23(1)$; $\delta = 1.22(1)$, $\Delta = 1.55(1)$, $\Gamma = 0.11(1)$ mm s$^{-1}$

**Table 4.** Major bond lengths (Å) in $FeCl_2 \cdot 4H_2O$, $CoCl_2 \cdot 6H_2O$, and $MnCl_2 \cdot 4H_2O$ crystal structures

| Complex | M–Cl | M–$OH_2$ | Ref. |
|---|---|---|---|
| $FeCl_2 \cdot 4H_2O$ | 2 at 2.38 | 2 at 2.59<br>2 at 2.09 | 25 |
| $CoCl_2 \cdot 6H_2O$ | 2 at 2.43 | 4 at 2.12 | 33 |
| $MnCl_2 \cdot 4H_2O$ | 2.475, 2.500 | 2.224, 2.209<br>2.185, 2.206 | 38 |

Table 1. Analyses were carried out by the Microanalytical Laboratory, Department of Chemistry, University of Manchester. The materials are extremely air-sensitive (to oxidation) and are handled under an $N_2$ atmosphere. *X*-Ray powder diffraction data of the products were obtained using a Philips 11.64 cm powder camera and Cu-$K_\alpha$ radiation.

The Mössbauer spectra were recorded on a Elscint MFD4 amplifier with a transducer driven by a home-built interface unit, counts being stored in an Intertechnique SA 40B analyser. The constant acceleration spectrometer was operated in a triangular wave-form mode. The source was ~8 mCi $^{57}$Co–Cu. The solid absorbers were finely powdered and sealed in a Perspex holder with Sellotape; the absorber thickness was *ca.* 0.02 g cm$^{-2}$. Velocity calibrations were carried out using thin 10 mg cm$^{-2}$ high-purity iron foils. The spectra were analysed by a simple non-linear least-squares fitting program; all isomer shifts are referred to natural iron.

## Results and Discussion

Mössbauer spectroscopic data are shown in Table 2 and Figures 1 and 2, and *X*-ray diffraction powder data in Table 3.

*The* Fe–Co *and* Fe–Ni *Chloride Tetrahydrate Systems.*—*Crystal structure of* $FeCl_2 \cdot 4H_2O$. This compound crystallizes in the monoclinic space group $P2_1/c$ with two molecules per unit cell.[25] The cell dimensions are $a = 5.91$, $b = 7.17$, $c = 8.44$ Å and $\beta = 112°$. A unit cell contains two equivalent $FeCl_2(H_2O)_4$ distorted octahedra related by a 180° rotation about the *b* axis. Each $FeCl_2(H_2O)_4$ has an $Fe^{II}$ environment in which the four $H_2O$ molecules are in a plane but the Fe–O bond lengths differ significantly,[15] with two *trans*-chloride ions making up the two other positions of the distorted octahedra.

The *X*-ray diffraction powder data show that the $M_xFe_{1-x}Cl_2 \cdot 4H_2O$ (M = Co or Ni; $x = 0.5$) phases are isomorphous with $FeCl_2 \cdot 4H_2O$ from which it may be presumed the phases are isostructural. The Mössbauer data however differ noticeably in quadrupole splitting from $FeCl_2 \cdot 4H_2O$, but only differ slightly in isomer shift, again showing that new single-phase solid solutions are present. The fact that the isomer shifts of these materials are similar indicates that the amount of 4*s* contribution to the bonding is nearly equal.

The quadrupole splitting data (Table 2) for $M_{0.5}Fe_{0.5}Cl_2 \cdot 4H_2O$ (M = Co or Ni) are similar, the Ni material having the slightly larger splitting. These data taken together with the nearly identical isomer shift data suggest that the $Fe^{II}$ environments are nearly identical and both have similar *p* and *d* electron participation in bonding.

The fact that the quadrupole splitting data for $M_{0.5}Fe_{0.5}Cl_2 \cdot 4H_2O$ (M = Co or Ni) are almost half the size of that of $FeCl_2 \cdot 4H_2O$ is striking, and to understand this it is first necessary to consider some fundamentals of quadrupole interactions.[32]

The free-ion configuration $^5D(^4t_{2g}{}^2e_g)$ for a high-spin $Fe^{2+}$ ion signifies a single 3*d* electron outside a spherical half-filled shell. In a ligand field possessing cubic symmetry, the $t_{2g}$ levels remain degenerate (as do the $e_g$) and there is no finite electric field gradient (e.f.g.).[32] However if the symmetry is lowered to tetragonal or trigonal, further degeneracy is removed. The sixth electron now occupies the lowest-lying unfilled state, and generates an e.f.g. at the nucleus. A ligand field of axial symmetry (*i.e.* a tetragonal distortion of the octahedron) will split the $t_{2g}$ state into a lower $d_{xy}$ single level and an upper $d_{xz}$, $d_{yz}$ state. The sixth electron now occupies the $d_{xy}$ level and will generate a quadrupole splitting in proportion to $V_{zz}/^e = q = (+4/7)\langle r^{-3}\rangle(1 - R)/(4\pi\varepsilon_0)$ where $R$ = 'atomic' Sternheimer factor, and $\varepsilon_0$ = permittivity of a vacuum. If the doublet $d_{xz}$, $d_{yz}$ state lies lowest the electron is in this state and gives $q = (-2/7)\langle r^{-3}\rangle(1 - R)/(4\pi\varepsilon_0)$. If the distortion is trigonal, the ground state corresponds to $d_{z^2}$ and gives $q = (-4/7)\langle r^{-3}\rangle(1 - R)/(4\pi\varepsilon_0)$.[32] From the *X*-ray powder diffraction data (Table 3) it is apparent that although the $Ni_{0.5}Fe_{0.5}Cl_2 \cdot 4H_2O$ and $Co_{0.5}Fe_{0.5}Cl_2 \cdot 4H_2O$ compounds are isostructural with $FeCl_2 \cdot 4H_2O$, their cell sizes are smaller showing that these

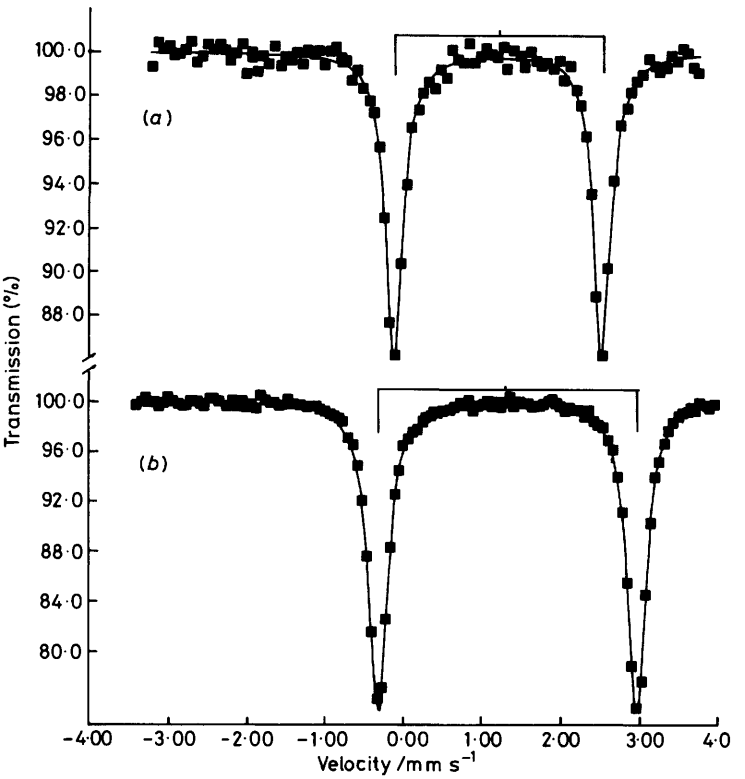


**Figure 2.** $^{57}$Fe Mössbauer spectra of $Mn_{0.5}Fe_{0.5}Cl_2\cdot4H_2O$ at (*a*) 298 and (*b*) 80 K

compounds are discrete phases and not mixtures of parent compounds (confirmed by different Mössbauer parameters). This obviously means that the $FeCl_2(H_2O)_4$ octahedra find themselves ' squeezed ' compared to the space available in the normal parent $FeCl_2\cdot4H_2O$ structure.[25] This squeezing generates the type of distortion responsible for changing the symmetry and gives rise to the much reduced quadrupole splitting.

Before considering this it is necessary to look at the known crystal structures in more detail. The major bond lengths found in the $FeCl_2\cdot4H_2O$ structure and those in $CoCl_2\cdot6H_2O$ [33] are shown in Table 4. The structure of $NiCl_2\cdot6H_2O$ is said to be isomorphous with that of $CoCl_2\cdot6H_2O$.[33] The M–$OH_2$ bond lengths are smaller in the Co and Ni structures although the M–Cl distances are slightly longer. Indeed it is of interest that the Fe–Cl bonds in $FeCl_2\cdot4H_2O$ [25] are considerably shorter than the sum of the ionic radii. It would seem likely that the Fe–Cl bonds are not squeezed in the $M_{0.5}Fe_{0.5}Cl_2\cdot4H_2O$ (M = Co or Ni) phases but that the ' average ' Fe–$OH_2$ bonds are. The observation that, in the parent $FeCl_2\cdot4H_2O$ structure, the Fe–Cl bonds are shorter than the sum of the ionic radii would be in keeping with a distorted tetragonal octahedron in which the $t_{2g}$ states are split into a lower $d_{xy}$ singlet and an upper $d_{xz}$, $d_{yz}$ state. The sixth electron now in the $d_{xy}$ will give rise to $q = (+4/7)\langle r^{-3}\rangle(1 - R)/(4\pi\varepsilon_0)$. For the $Ni_{0.5}$ and $Co_{0.5}$ materials the squeezing is likely to occur in the Fe–$OH_2$ bonds and this would generate a tetragonal distortion in which the $t_{2g}$ states are split into a lower doublet $d_{xy}$, $d_{yz}$ state and an upper singlet $d_{xy}$ state. The odd electron is now in the doublet state and $q = (-2/7)\langle r^{-3}\rangle(1 - R)/(4\pi\varepsilon_0)$. Thus the quadrupole splitting for the $Ni_{0.5}$ and $Co_{0.5}$ materials would be expected to be about half that observed for $FeCl_2\cdot4H_2O$.

The fact that the quadrupole splittings observed for the $Ni_{0.5}$ and $Co_{0.5}$ materials are slightly different reflects slight differences in the covalent contributions to the bonding in the $FeCl_2(H_2O)_4$ unit caused by the slightly different extents of squeezing in these two materials. It must be noted here that although slight differences in quadrupole splittings may be caused by such differences in covalency effects, the quadrupole splitting itself originates from the sensitivity of the orbital state of an essentially non-bonding electron to the geometrical environment.[32]

The isomer shifts for the $M_xFe_{1-x}Cl_2\cdot4H_2O$ (M = Co or Ni; $x = 0.5$) materials at 298 and 80 K are both slightly less than that of $FeCl_2\cdot4H_2O$, although in both, the $Fe^{II}$ has *trans* chlorides. This change in isomer shift is in keeping with the work of Drickamer and co-workers [30] in which they predict an increase in electron density at the iron nucleus with pressure and a decrease in chemical shift. This would be consistent with a reduction in 3*d* shielding. In these materials however we do not see an increase in quadrupole splitting, in contrast to Drickamer's pressure experiments.

Similar changes of quadrupole splitting for $FeCl_2(H_2O)_4$ octahedra have been reported by other workers. Ruby *et al.*[34,35] reported a quadrupole splitting of 1.6 mm $s^{-1}$ for a frozen solution (assumed to be $FeCl_2\cdot6H_2O$) after annealing at 225 K where crystallization takes place. This compares to a quadrupole splitting of 3.4 mm $s^{-1}$ for $FeCl_2\cdot6H_2O$ on quench freezing to a glass. Indeed conversion from glass to crystal on annealing would be accompanied by a decrease in volume, and is also accompanied by a change in the quadrupole splitting from 3.4 to 1.6 mm $s^{-1}$ for $FeCl_2\cdot6H_2O$. Significantly, in both the Fe–Co and Fe–Ni systems the $FeCl_2$ rich end shows a splitting of 3.0 mm $s^{-1}$, typical of normal $FeCl_2\cdot4H_2O$.

The Fe–Co system was studied in detail (see Table 2). Although any $Fe_xCo_{1-x}$ ($x = 0$—1) ratio may be prepared only three different Mössbauer spectra are ever obtained in the system. This shows that only three electronically different $Fe^{II}$ environments are present. Materials with excess $FeCl_2\cdot4H_2O$ only showed the Mössbauer parameters of the

parent $FeCl_2 \cdot 4H_2O$. Thus the $CoCl_2(H_2O)_4$ octahedra appear to sit randomly in the lattice for concentrations below *ca.* 30% $CoCl_2$ without squeezing the $Fe^{II}$ environments. The two other Mössbauer spectra are found in materials with 50% or greater $CoCl_2$. The quadrupole splittings of 1.6 mm $s^{-1}$ (already discussed) and 2.64 mm $s^{-1}$ are both associated with distorted octahedral electronic environments.

In studies on perovskite caesium tin(II) halides [36,37] it was found that gradual changes in the cell size were accompanied by gradual changes in the Mössbauer isomer shift. In the Fe–Ni and Fe–Co systems we do not find gradual changes in the cell size; above 50% $CoCl_2$ the structure found predominating is that of the parent $CoCl_2 \cdot 6H_2O$ but the cell size (from *X*-ray powder data) is larger.

The chemical analyses (not presented here) for phases above 50% $CoCl_2$ are not easily fitted to one discrete formula. In agreement with the Mössbauer data which show two $Fe^{II}$ environments (Table 2, Figure 1) one of which is that of the $Co_{0.5}Fe_{0.5}Cl_2 \cdot 4H_2O$ phase, the analyses give evidence for more than one compound and *X*-ray powder diffraction data confirm the presence of two phases. Consequently, the Mössbauer site with a quadrupole splitting of 2.65 mm $s^{-1}$ is simply noted here as being found in an environment that is at least $MCl_2 \cdot 4H_2O$ and may be $MCl_2 \cdot 6H_2O$, but for lack of definite assignment is not discussed further.

The fact that only two $Fe^{II}$ sites persist in the $Fe_xM_{1-x}Cl_2 \cdot 6H_2O$ (M = Co or Ni, $x \leq 0.5$) system suggests that only H-bonding between $MCl_2(H_2O)_4$ octahedra is important in packing (and/or squeezing) the octahedra (as is suggested for $FeCl_2 \cdot 4H_2O$ [17]). The hydrogen bond lengths do not change gradually with increase of percentage $CoCl_2 \cdot 6H_2O$ (or $NiCl_2 \cdot 6H_2O$).

*The* Fe–Mn *Chloride Tetrahydrate System.*—The $Mn_xFe_{1-x}Cl_2 \cdot 4H_2O$ system differs significantly from those of Fe–Co and Fe–Ni. The $Mn^{II}$ is larger than $Fe^{II}$ and the structure of $MnCl_2 \cdot 4H_2O$ contains *cis* chlorides on the $Mn^{II}$ octahedra.

However, $MnCl_2 \cdot 4H_2O$ is considered to be isomorphous with $FeCl_2 \cdot 4H_2O$ except for the chloride positions.[38] The *X*-ray powder diffraction data (Table 3) show that $Fe_{0.5}Mn_{0.5}Cl_2 \cdot 4H_2O$ is isostructural with $MnCl_2 \cdot 4H_2O$. Only one new Mössbauer spectrum was found in this system (Figure 2); the chemical shift is similar to that found for $FeCl_2 \cdot 4H_2O$ but the quadrupole splitting is smaller at room temperature, but much larger at 80 K. This is the only system which shows a significant temperature dependence of the quadrupole splitting; this change is gradual and rules out a phase change.

At a very high temperature, all the levels of the $t_{2g}$ multiplet would be equally populated by thermal excitation, and the e.f.g. would be zero. The temperature dependence of the quadrupole splitting in the Mn–Fe system is primarily due to the Boltzman population of the $d^6$ manifolds.[32] A partial degree of thermal excitation will cause a partial cancellation of the e.f.g., so that the quadrupole splitting should decrease with rise in temperature. A full mathematical treatment of the temperature dependence is given by Ingalls.[39] The limiting value of the quadrupole splitting (3.3 mm $s^{-1}$ in this case) at low temperature relates to the orbital state of the lowest lying levels (by comparison with $FeCl_2 \cdot 4H_2O$ a singlet state) and the significant decrease with increasing temperature relates to the population of many low lying excited states. This compares to $FeCl_2 \cdot 4H_2O$ which shows little temperature dependence of the quadrupole splitting over a similar temperature range and presumably signifies that in this compound the excited states are separated by greater energies from the ground state.

As $Mn^{II}$ is larger than $Fe^{II}$ so it might be expected that the $Fe^{II}$ in the $Mn^{II}$ rich materials [where the quadrupole splitting of 2.6 mm $s^{-1}$ is observed at 298 K (Figure 2)] is in a larger hole than usual. The electronic environments might be expected to be more symmetric, as the crystal field splitting would be smaller; this will give rise to a more compact array of excited states with a smaller range of energy differences as is observed in the temperature behaviour of the quadrupole splitting.

The room temperature spectrum of the $Fe^{II}$ site in the Fe–Mn materials which shows a weaker crystal field than found in $FeCl_2 \cdot 4H_2O$ may be caused indirectly by the $Mn^{II}$ octahedra which contain *cis* chloride ions. There is no evidence (from *X*-ray powder data) to suggest that the $Fe^{II}$ site does not still have *trans* chloride ions. One explanation may be that hydrogen bonding between differing octahedra distorts the $Fe^{II}$ environments at room temperature less than in the parent $FeCl_2 \cdot 4H_2O$ where all octahedra have *trans* chloride ions.

Another major factor that may influence the quadrupole splitting is the temperature dependence of the ligand field splittings and the lattice term caused as a direct result of thermal expansion. The only parameters one could expect to change gradually with temperature would be the lattice cell constants. Therefore the decrease in quadrupole splitting could also be related to increasing cell size.

It is obviously significant that the large quadrupole splitting of *ca.* 3.3 mm $s^{-1}$ is close to those found for materials containing $[Fe(H_2O)_6]^{2+}$ octahedra, and must mean that at 80 K the electronic environment in the Fe–Mn material is similar to that found for the $[Fe(H_2O)_6]^{2+}$ species although the environment in this material is $FeCl_2(H_2O)_4$ with *trans* chlorines. Frozen aqueous solutions of iron(II) salts have been studied by Mössbauer spectroscopy and other methods.[40–46] In these systems the $Fe^{2+}$ ion forms an $[Fe(H_2O)_6]^{2+}$ complex. The distortion of the $[Fe(H_2O)_6]^{2+}$ octahedra is mainly determined by the $[Fe(H_2O)_6]^{2+}$ complex itself,[46] and it is likely that a similar distortion in the $FeCl_2(H_2O)_4$ octahedra is similarly determined.

The gradual decrease of the quadrupole splitting of the material in the Fe–Mn system must therefore be caused either by less distortion of the ligand electronic field as the lattice expands, or changes in the symmetry of the *d* electron distribution imposed by the $Fe^{2+}$ ion itself.

It is also worth noting that the Fe–Mn material never shows quite the same parameters for both isomer shift and quadrupole splitting that the parent $FeCl_2 \cdot 4H_2O$ exhibits. In the quadrupole splitting range between 80 and 300 K for $FeCl_2 \cdot 4H_2O$ (3.10—2.99 mm $s^{-1}$) the isomer shift is 1.33—1.22 mm $s^{-1}$, for the Fe–Mn material in the same isomer shift range the quadrupole splitting range is 3.29—2.60 mm $s^{-1}$. This indicates that the two $Fe^{II}$ environments are always slightly different, suggesting that the $FeCl_2(H_2O)_4$ octahedron is never identical to that of the parent structure. However, because of the method of preparation it is not likely that the chloride ions in the $Fe^{II}$ octahedra are *cis*.

The fact that the isomer shifts at 80 and at 298 K are so similar for the Fe–Mn material and $FeCl_2 \cdot 4H_2O$ according to Drickamer's argument [30] would confirm that there are no significant pressure differences in these two systems.

The only other major factor which could affect the e.f.g. tensor in these systems is the 'lattice' term contribution. However, because of the similar overall sizes of the $MCl_2(H_2O)_4$ octahedra this term should be of similar size in the systems studied here and should thus contribute to a similar extent in all the Mössbauer spectra and so can be neglected as a cause for the differences recorded in this work.

## Conclusions

The results found in the Fe–Co and Fe–Ni systems studied in this work can be explained in terms of squeezing of the Fe–

$OH_2$ bonds causing the $t_{2g}$ states to split into a lower $d_{xz}$, $d_{yz}$ doublet, whereas in the parent compound $FeCl_2 \cdot 4H_2O$ it is a singlet. The Fe–Mn system also gives results which appear to be directly related to volume changes but no evidence is found for pressure effects.

Thus the systems reported here behave quite differently to the cubic $KFe_xM_{1-x}F_3$ systems.[26,27] In the $KFe_xM_{1-x}F_3$ systems the $M^{II}$ ions (M = Mn, Co, or Ni) lower the electronic degeneracy of the $Fe^{II}$ ions producing an e.f.g. of sufficient size to give quadrupole splitting.[27] In this work the different transition metals are further away from the $Fe^{II}$ sites and their different electronic environments (due to different *d* orbital populations) are considered to have little effect on the quadrupole splitting observed.

## Acknowledgements

We thank Dr. L. V. C. Rees of the Department of Chemistry, Imperial College, for Mössbauer facilities, and Dr. J. R. Miller of this Department for useful discussions.

## References

1 R. W. Grant, H. Wiedersich, A. H. Muir, U. Gonser, and W. N. Delgass, *J. Chem. Phys.*, 1966, **45**, 1015.
2 K. Ono, M. Shinohara, A. Ito, T. Fujita, and A. Ishigaki, *J. Appl. Phys.*, 1968, **39**, 1126.
3 C. D. Burbridge and D. M. L. Goodgame, *J. Chem. Soc. A*, 1968, 1410.
4 A. J. Nozik and M. Kaplan, *J. Chem. Phys.*, 1967, **47**, 2960.
5 J. V. Dilorenzo and M. Kaplan, *Chem. Phys. Lett.*, 1969, **3**, 216.
6 C. E. Johnson and M. S. Ridout, *J. Appl. Phys.*, 1967, **38**, 1272.
7 P. Zory, *Phys. Rev.*, 1965, **140**, A1401.
8 A. J. Nozik and M. Kaplan, *Phys. Rev.*, 1967, **159**, 273.
9 S. Chandra and G. R. Hoy, *Phys. Lett.*, 1966, **22**, 254.
10 C. E. Johnson, *Proc. Phys. Soc., London*, 1966, **88**, 943.
11 G. Ziebarth, *Z. Phys.*, 1968, **212**, 330.
12 A. Vertes, T. Szekely, and T. Tarnoczy, *Acta Chim. Acad. Sci. Hung.*, 1970, **63**, 1.
13 A. Vertes, *Acta Chim. Acad. Sci. Hung.*, 1970, **63**, 9.
14 G. A. Sawatzky and F. Van Der Woude, *Chem. Phys. Lett.*, 1969, **4**, 335.
15 B. Brunot, *J. Chem. Phys.*, 1974, **6**, 2360.
16 T. C. Gibb, *Chem. Phys.*, 1975, **7**, 449.
17 M. Shinohara, *J. Phys. Soc. Jpn.*, 1977, **42**, 65.
18 W. Siebke, S. Hosl, H. Spiering, and G. Ritter, Proc. Conf. Mössbauer Spectroscopy, Bratislava, 1973, p. 176.
19 H. Spiering, S. Hosl, and H. Vogel, *Phys. Status Solidi B*, 1978, **85**, 87.
20 H. Spiering and H. Vogel, *Hyperfine Interact.*, 1977, **3**, 221.
21 R. Zimmermann, *Nucl. Instrum. Methods*, 1975, **128**, 537.
22 I. O. Suzdalev and A. P. Amulyavichus, *Zh. Eksp. Teor. Fiz.*, 1971, **61**, 2354.
23 J. Tatarkiewez, *Postepy. Fiz.*, 1976, **26**, 641.
24 B. Morosin and E. J. Graeber, *J. Chem. Phys.*, 1965, **42**, 898.
25 B. R. Penfold and J. A. Grigor, *Acta Crystallogr.*, 1959, **12**, 850.
26 J. Silver, *J. Fluorine Chem.*, 1976, **8**, 527.
27 J. Silver and J. D. Donaldson, *Inorg. Nucl. Chem. Lett.*, 1976, **12**, 795.
28 R. Fatehally, G. K. Shenoy, N. P. Sastry, and R. Nagarajan, *Phys. Lett. A*, 1967, **25**, 453.
29 E. Simanek and A. Y. C. Wong, *Phys. Rev.*, 1968, **166**, 348.
30 A. R. Champion, R. W. Vaughan, and H. G. Drickamer, *J. Chem. Phys.*, 1967, **47**, 2583.
31 L. R. Walker, G. K. Wertheim, and V. Jaccarino, *Phys. Rev. Lett.*, 1961, **6**, 98.
32 ' Principles of Mössbauer Spectroscopy,' T. C. Gibb, Chapman and Hall, London, New York, 1976.
33 J. Muzuno, *J. Phys. Soc. Jpn.*, 1960, **15**, 1412.
34 S. L. Ruby and B. L. Zabransky, *Chem. Phys. Lett.*, 1972, **13**, 382.
35 S. L. Ruby, B. L. Zabransky, and J. G. Stevens, *J. Chem. Phys.*, 1971, **54**, 11.
36 J. D. Donaldson and J. Silver, *J. Chem. Soc., Dalton Trans.*, 1973, 666.
37 J. D. Donaldson, D. Laughlin, S. D. Ross, and J. Silver, *J. Chem. Soc., Dalton Trans.*, 1973, 1985.
38 A. Zalkin, J. D. Forrester, and D. H. Templeton, *Inorg. Chem.*, 1964, **3**, 529.
39 R. Ingalls, *Phys. Rev. A*, 1964, **133**, 787.
40 I. Dezsi, L. Keszthelyi, L. Pocs, and L. Korecz, *Phys. Lett.*, 1965, **14**, 14.
41 I. Dezsi, L. Keszthelyi, B. Molnai, and L. Pocs, *Phys. Lett.*, 1965, **18**, 28.
42 A. J. Nozik and M. Kaplan, *Chem. Phys.*, 1967, **47**, 2960.
43 J. V. Di Lorenzo and M. Kaplan, *Chem. Phys. Lett.*, 1968, **2**, 509.
44 I. Dezsi, L. Keszthelyi, G. Nagy, and D. L. Nagy, Proc. Conf. Appl. Mössbauer Effect, Tihany, 1969, ed. I. Dezsi, Akademiai, Budapest, 1971, p. 607.
45 G. Nagy, L. Kacsoh, J. Nyest, and I. Dezsi, *J. Thermal Anal.*, 1972, **4**, 257.
46 D. L. Nagy, J. Balogh, I. Dezsi, G. Ritter, H. Spiering, and H. Vogel, *J. Phys. (Paris), Colloq.*, 1980, **41**, Cl-283.

*Received* 8*th March* 1982; *Paper* 2/400